

Lasing with coherent feedback in weak scattering media

X. Wu¹, W. Fang¹, A. Yamilov^{1,2}, A. A. Chabanov^{1,3}, and H. Cao¹

¹ *Department of Physics and Astronomy,*

Northwestern University, Evanston, Illinois, 60208.

² *Department of Physics, University of Missouri-Rolla, Rolla, Missouri, 65409.*

³ *Department of Physics and Astronomy,*

University of Texas-San Antonio, San Antonio, Texas, 78249.

Abstract

We present detailed experimental and numerical studies of lasing with coherent feedback in weakly scattering systems. The interference effects, which are weak in the passive systems, are strongly enhanced by coherent amplification in the active systems. The lasing modes are confined in the vicinity of the excited volume due to absorption of emitted light outside it. In the ballistic regime where the size of gain volume is less than the scattering mean free path, lasing oscillation occurs along the direction in which the gain volume is most extended, producing directional laser output. The feedback for lasing originates mainly from backscattering of particles near the boundaries of pumped region, because its longest length of one path across the gain volume leads to most amplification. It results in regular frequency spacing of lasing modes, which scales inversely with the maximum dimension of the gain volume.

PACS numbers: 42.55.Zz,42.25.Dd

I. INTRODUCTION

Since the pioneering work of Letokhov and coworkers¹, lasing in disordered media has been a subject of intense theoretical and experimental studies². It represents the process of light amplification by stimulated emission with feedback mediated by random fluctuation of dielectric constant in space. There are two kinds of feedback: one is *intensity* or *energy* feedback, the other is *field* or *amplitude* feedback². The field feedback is phase sensitive (i.e. coherent), and therefore frequency dependent (i.e. resonant). The intensity feedback is phase insensitive (i.e. incoherent) and frequency independent (i.e. non-resonant). Based on the feedback mechanisms, random lasers are classified into two categories: (i) random lasers with incoherent and non-resonant feedback, (ii) random laser with coherent and resonant feedback.

Over the past few years, there have been many studies on random lasers with coherent feedback³. In our previous experiments with highly disordered semiconductor powder and polycrystalline films, the transport mean free path was short, and recurrent scattering provided field feedback for lasing⁴. When the optical gain was sufficient, lasing oscillation occurred at discrete frequencies that were determined by the interference of multiply scattered light. However, lasing with coherent feedback was realized also in weakly scattering random media^{5,6,7,8,9}. The coherent feedback mechanism relies on the interference effect, which is expected to be small in the weak scattering regime. That is why the phase of electromagnetic field is ignored in the diffusion equation for intensity. In this paper, however, we demonstrate that the interference effect is dramatically enhanced in the presence of high gain, leading to lasing with coherent feedback in weakly scattering systems. Strong coherent amplification of field feedback can result in lasing in the ballistic regime where the size of gain volume is less than the scattering mean free path, i.e., the feedback originating from single particle scattering may be enough for lasing under intense pumping.

In our previous paper¹⁰, we illustrated with numerical simulations that the lasing modes in weakly scattering system may be spatially localized. The localization is caused not by strong scattering, but by absorption of emitted light outside the pumped region. The reabsorption of emission suppresses the feedback from the unpumped part of the random system and effectively reduces the system size. The lasing modes are therefore drastically different from the quasimode of the passive system (without gain or absorption). Even if all the

quasimodes of the passive system are extended across the entire system, the lasing modes are still confined in the vicinity of the gain volume. In this paper, we provide a direct experimental proof for the absorption-induced localization of lasing modes. Our results also indicate that when the size of gain volume is less than the scattering mean free path, the lasing modes may be different from the quasimodes of the *reduced* system. In the absence of gain, the quasimodes are formed by scattering of all particles inside the reduced system. In contrast, the lasing modes are formed mainly by scattering of particles near the boundary of the reduced system when the optical gain is very high.

The paper is organized as follows. In section II, a detailed experimental study of lasing in weakly scattering systems is presented. The feedback mechanism is demonstrated via simplified numerical simulations in Section III. Section IV has a brief discussion and conclusion.

II. EXPERIMENTS

We have performed experiments on several weakly-scattering systems which consist of passive scatterers embedded in active homogeneous media. The scatterers are TiO_2 particles of radius 200 nm, ZnO particles of radius 38 nm, SiO_2 particles of radius 220 nm. The nanoparticles are suspended in a laser dye solution, e.g., Rhodamine 640 perchlorate or Rhodamine 590 chloride in diethylene glycol (DEG) or methanol. The experimental results obtained with different particles, dyes and solvents are qualitatively similar. As an example, we will demonstrate the lasing phenomena with colloidal suspensions of TiO_2 particles in DEG with Rhodamine 640.

A small amount of TiO_2 (rutile) particles, with an average radius of 200 nm, were dissolved in the DEG solution of rhodamine 640 perchlorate dye. To prevent flocculation, the TiO_2 particles were coated with a thin layer of Al_2O_3 . DEG was chosen as the solvent instead of the widely-used methanol because of the facts that (i) the windows of the quartz cuvette that contained the methanol solution were coated with a layer of TiO_2 particles, whereas such coating was not observed for the DEG solution; (ii) the viscosity of DEG is about 30 times larger than methanol, thus the sedimentation of TiO_2 particles in DEG is much slower. In our experiment, the particle density ρ ranged from $1.87 \times 10^8 \text{ cm}^{-3}$ to $5.6 \times 10^{10} \text{ cm}^{-3}$. The scattering mean free path was estimated by $l_s = 1/\rho\sigma_s$, where σ_s is the scattering

cross section of a TiO_2 spherical particle with radius 200 nm. The value of l_s varied from 1.07 cm to 35 μm . The dye molarity M also changed from 3 to 10 mM. Right before the lasing experiment, the suspension was placed in an ultrasonic bath for 30 minutes to prevent sedimentation of the particles. During the experiment, the solution was contained in a quartz cuvette that was 1.0 cm long, 1.0 cm wide and 4.5 cm high. The dye molecules in the solution were optically pumped by the frequency-doubled output ($\lambda_p = 532$ nm) of a mode-locked Nd:YAG laser (25 ps pulse width, 10 Hz repetition rate). The pump beam was focused by a lens into the solution through the front window of the cuvette. The radius of the pump spot at the entrance to the solution was about 20 μm . The experimental setup is shown schematically in the inset of Fig. 1. The emission from the solution was collected in the backward direction of the incident pump beam. A second lens focused the emission into a fiber bundle (FB) which was connected to the entrance slit of a spectrometer with cooled CCD array detector. The spectral resolution was 0.06 nm.

We started the experiment with a sample of $M = 5$ mM and $\rho = 3.0 \times 10^9$ cm^{-3} . At low pumping level, the emission spectrum featured the broad spontaneous emission band of rhodamine 640 molecules. Above a threshold pump intensity, discrete narrow peaks emerged in the emission spectrum, and their intensities grew rapidly with increasing pumping. This behavior corresponded to the onset of lasing. The lasing peaks could be as narrow as 0.12 nm. Their frequencies changed from pulse to pulse (shot). We repeated the experiment with samples of different particle density but the same dye concentration. Lasing was observed only within certain range of particle density. Figure 1 show the spectra of emission from five samples taken at the same incident pump pulse energy 0.4 μJ . Each spectrum was integrated over 25 shots. Only a relatively broad amplified spontaneous emission (ASE) peak was observed for the neat dye solution, whereas a few discrete lasing peaks emerged on top of the ASE spectrum at small particle concentration $\rho = 1.87 \times 10^8$ cm^{-3} . Increasing particle density to 1.87×10^9 cm^{-3} led to an increase in the number of lasing peaks and the peak intensity. However, when ρ increased further to 1.3×10^{10} cm^{-3} , the lasing emission started to decrease. Eventually at $\rho = 5.0 \times 10^{10}$ cm^{-3} lasing peaks disappeared. A further increase of the incident pump pulse energy to 1.2 μJ resulted in an ASE peak at longer wavelength, shown in the right inset of Fig. 1. The red shift of the ASE peak might be caused by the surface effect on emission frequency of Rhodamine 640 molecules adsorbed on the TiO_2 particles. One support for this explanation was that the emission frequency was

blue shifted when we replaced the TiO_2 particles by SiO_2 particles.

In Fig. 2, the incident pump pulse energy at the lasing threshold P_t is plotted against the particle density ρ . At the lasing threshold, the slope of emission intensity versus pump pulse energy exhibited a sudden increase (inset of Fig. 2). At $\rho = 3.8 \times 10^8 \text{ cm}^{-3}$, lasing started at $0.21 \mu\text{J}$. As ρ increased to $1.5 \times 10^9 \text{ cm}^{-3}$, P_t decreased gradually to $0.12 \mu\text{J}$. Then it remained nearly constant with a further increase of ρ . The threshold started to rise at $\rho = 1.9 \times 10^{10} \text{ cm}^{-3}$, then went up quickly with ρ . At $\rho = 5.6 \times 10^{10} \text{ cm}^{-3}$, no lasing peaks were observed up to the maximum pump pulse energy $2.0 \mu\text{J}$ we used, although at $1.0 \mu\text{J}$ an ASE peak appeared at longer wavelength.

The threshold behavior illustrated that lasing in the dilute suspension of particles was very different from random lasing in strongly-scattering systems. In the latter, the lasing threshold decreases with an increase in the amount of scattering². However, the particles must play an essential role in the former lasing process because it did not happen in the neat dye solution. One possibility was lasing within individual particles that served as laser resonators. It contradicted two experimental observations: (i) the lasing threshold depended on the particle density (Fig. 2); (ii) the lasing emission was highly directional (shown next). The left inset of Fig. 3 is a sketch of our directionality measurement setup. A fiber bundle was placed at the focal plane of the lens. It was scanned with fine steps parallel to the focal plane. At each step, the spectrum of emission into a particular direction was recorded. The emission angle θ was computed from the fiber bundle position. Its range was limited by the diameter of the lens to about 14 degree. $\theta = 0$ corresponded to the backward direction of the incident pump beam. In each spectrum, the emission intensity was integrated over the wavelength range of $604 - 612 \text{ nm}$ in which the lasing peaks were located. Figure 3 is a plot of the integrated emission intensity versus the output angle θ at $\rho = 3.0 \times 10^9 \text{ cm}^{-3}$. Although the spontaneous emission at low pumping was isotropic, the lasing emission was strongly confined to the backward direction of the incident pump beam. The divergence angle $\Delta\theta$ of the output laser beam was merely 4 degree. To check the effect of reflection by the front window of the cuvette on lasing, we rotated the cuvette around the vertical axis and repeated the measurement. As shown in the right inset of Fig. 3, ϕ represented the angle between the incident pump beam and the normal of the front window. Similar lasing phenomena were observed except a slight increase of the lasing threshold. The lasing emission was always confined to the backward direction of pump beam even when ϕ was

much larger than the divergence angle of the focused pump beam, which was about 4 degrees. This result demonstrated that the front window of the cuvette did not play an essential role in the lasing process. Figure 3 also shows the angular distribution of ASE from a sample of higher particle density ($\rho = 5 \times 10^{10} \text{ cm}^{-3}$). The integrated intensity of ASE (at longer wavelength) was nearly constant over the angular range of detection.

To understand the directionality of lasing emission from the dilute suspension, the pumped region was imaged through a side window of the cuvette. The measurement setup is sketched in the inset of Fig. 4(a). Emission from the excited region was collected through the side window by a 5x objective lens and imaged onto a CCD camera by integrating multiple pulses. Spectrum was taken simultaneously by partitioning the signal with a beam splitter (BS). Figure 4(a) compares the spectrum of emission through the side window to that through the front window of the cuvette from the same sample ($\rho = 3 \times 10^9 \text{ cm}^{-3}$, $M = 5 \text{ mM}$) under identical pumping condition. The spectrum of emission from the front window exhibited large lasing peaks. However, only spontaneous emission was observed through the side window, and it shifted to longer wavelength as a result of reabsorption in the unpumped solution between the excited region and side window. To calibrate the reabsorption, we measured the spontaneous emission spectra at low pumping from both front and side windows. The magnitude of reabsorption was estimated from the intensity ratio of emission through the side window to that through the front. Based on this estimation, we concluded that the absence of lasing peaks in the side emission spectrum at high pumping was not caused by reabsorption. This conclusion was in agreement with the directionality measurement result presented in the Fig. 3. More importantly, the image of spontaneous emission intensity distribution taken through the side window exhibited the shape of the excited region in the sample. As shown in Fig. 4(b), the excited volume at low particle density had a cone shape. The length of the cone was much larger than its base diameter. Unfortunately, we could not get the exact length of the cone from the image, because near its end the spontaneous emission was too weak to be recorded by the CCD camera. At high particle density, the shape of excited volume changed to hemisphere as shown in Fig. 4(c) at a higher pumping power. This change was caused by increased scattering of pump light. In Fig. 4(b) $\rho = 3.0 \times 10^9 \text{ cm}^{-3}$, the scattering mean free path l_s at the pump wavelength $\lambda_p = 532 \text{ nm}$ was estimated to be $800 \mu\text{m}$. The (linear) absorption length l_a , obtained from the transmission measurement of neat dye solution, was about $50 \mu\text{m}$ at $\lambda_p = 532 \text{ nm}$.

Strong pumping in the lasing experiment could saturate the absorption of dye molecules, leading to an increase of l_a . Since the shape of the excited volume shown in Fig. 4(b) was nearly identical to that in the neat dye solution, the scattering of pump light must be much weaker than absorption, i.e., l_a was still shorter than l_s . In Fig. 4(c) $\rho = 5.0 \times 10^{10} \text{ cm}^{-3}$, l_s was shortened to $53 \text{ }\mu\text{m}$. Scattering of pump light became much stronger. As a result of multiple scattering, the cone was replaced by a hemisphere. The image of excited volume provided some clue to high directionality of lasing emission at small ρ and non-directionality of ASE at large ρ in Fig. 3. At low particle density, stimulated emission in the cone-shaped gain volume was the strongest along the cone due to the longest path length. Since the cone was parallel to the incident pump beam, lasing was confined to the direction parallel to the pump beam. The divergence angle $\Delta\theta$ of laser output was determined by the aspect ratio of the excited cone, namely, $\Delta\theta \sim 2r_p/L_p$, where L_p is the cone length and r_p is the base radius. At large ρ , emitted photons experienced multiple scattering while being amplified in the hemisphere-shaped gain volume. Hence, the ASE was nearly isotropic.

Therefore, the shape of gain volume determined the lasing directionality, i.e., lasing occurred along the direction in which the gain volume was most extended. However, it was still not clear how the laser cavities were formed in the dilute suspension, in other words, where the coherent feedback for lasing came from. We examined the lasing spectra more carefully by taking single-shot emission spectra with the setup shown in the inset of Fig. 1. Surprisingly, in most single-shot spectra the lasing peaks were almost equally spaced in frequency. Figure 5(a) is an example of single-shot emission spectrum taken from the sample of $\rho = 1.87 \times 10^9 \text{ cm}^{-3}$ and $M = 5 \text{ mM}$. The spectral correlation function $C(\Delta\lambda) \equiv \langle I(\lambda)I(\lambda + \Delta\lambda) \rangle / \langle I(\lambda)^2 \rangle$ was computed for the spectrum in Fig. 5(a) and plotted in Fig. 5(b). The regularly spaced correlation peaks revealed the periodicity of lasing peaks. Despite that the lasing peaks completely changed from shot to shot, the peak spacing was nearly the same. In the spectrum taken over many shots, the periodicity was smeared out due to random (uncorrelated) peak positions in different shots. As an example, in Fig. 1 the lasing spectra (curve 3) were integrated over 25 pulses and the lasing peaks did not exhibit clear periodicity. We also noticed that the periodicity was less obvious at higher particle density.

We would like to point out that the lasing peaks in the dilute suspension of particles are fundamentally different from the stochastic ASE spikes that could be observed even in

the neat dye solution. Figure 6 shows a single-shot spectrum of emission from the DEG solution of 5 mM Rhodamine 640 without any particles. The spectrum was taken under the same condition as that in Fig. 5. At high pumping level, stochastic spikes appeared on top of the ASE peak. The spikes in Fig. 6 were much denser and narrower than the lasing peaks in Fig. 5. They changed constantly from shot to shot. When integrating the spectrum over subsequent shots, the spikes were quickly averaged out, leaving a smooth ASE spectrum shown as curve 1 in Fig. 1. Unlike the lasing peaks, the stochastic spectral structures of ASE was rather ubiquitous. We varied the dye molarity, changed the solvent, and tried a different dye LDS722. The emission spikes always appeared when the pumping was high enough. However, lasing peaks were not observed in some of these dye solutions when TiO_2 particles were added. Note that the stochastic spikes also appeared in the spectrum of emission from the dye solutions with particles. However, they were taken over by the huge lasing peaks at high pumping level. The stochastic structure of the pulsed ASE spectrum was reported thirty years ago^{11,12}. Since then, there have been detailed experimental and theoretical studies on this phenomenon^{13,14,15,16}. The spectral fluctuation originated from random spontaneous emission at one end of the cone-shaped pump volume. It was strongly amplified as it propagated through the cone. Non-stationary interference of the partially coherent ASE not only presented a grainy spatial pattern, but also caused drastic temporal fluctuation of intensity. The random intensity fluctuation within an ASE pulse in the time domain generated stochastic spikes in the spectral domain. According to the Fourier transformation, the width of spectral spikes was inversely proportional to the ASE pulse duration. In our case of picosecond pumping, the ASE pulse duration was of the order 25 ps. Thus the average spike width should be ~ 0.05 nm, which was close to the measured value of 0.07 nm.

To find out the location and size of the laser cavities in the dilute suspension, we placed a metallic rod in between the excited volume and the back window (inset of Fig. 7). On one hand, the rod prevented the emission from being reflected by the back window into the gain volume. On the other hand, a Fabry-Perot cavity was formed by the rod and the front window. Lasing in this cavity produced equally spaced peaks in the emission spectrum. The peak spacing $\Delta\lambda$ was determined by the cavity length d (the distance between the rod and the front window), $\Delta\lambda = \lambda^2/2n_e d$, where n_e is the effective index of suspension. As plotted in Fig. 7, $\Delta\lambda$ decreased with increasing d . However, when d exceeded a critical

value $d_0 \simeq 450 \mu\text{m}$, $\Delta\lambda$ jumped to a constant value and did not change with d any more (Fig. 7). The lasing spectrum and peak spacing at $d > d_0$ were identical to those from the same sample without the metallic rod. This result demonstrated that the laser cavity in the colloidal solution was located within $450 \mu\text{m}$ from the front window, i.e., in the vicinity of excited cone. Despite the scattering mean free path $l_s \sim 800 \mu\text{m}$ much larger than the wavelength, the laser cavity was not extended over the entire sample, but confined to a region of dimension less than l_s . This is due to reabsorption of laser emission in the unpumped part of sample. Our white-light absorption measurement and photoluminescence measurement of neat dye solution showed that Rhodamine 640 molecules in DEG had significant overlap between the absorption band and emission band. At the dye concentration $M = 5 \text{ mM}$, the absorption length at the emission wavelength $\lambda_e \sim 610 \text{ nm}$ was about $300 \mu\text{m}$. When the density of TiO_2 particles in the solution was low, the absorption length of emitted photons in the unpumped region was shorter than the scattering length. Once an emitted photon left the pumped region, the chance of coming back after multiple scattering was extremely low. Therefore, the reabsorption of emission suppressed the feedback from the unpumped region of the system, and effectively reduced the system (or cavity) size¹⁰.

The above experiment illustrated the laser cavity was confined in the vicinity of the excited region as a result of the interplay between amplification and reabsorption. The directionality of laser output suggested the laser cavity was oriented along the excited cone. Using the formula of a Fabry-Perot cavity, we derived the cavity length L_c from the wavelength spacing $\Delta\lambda$ of the lasing peaks, $L_c = \lambda^2/2n_e\Delta\lambda \sim 200 - 300 \mu\text{m}$. The estimated cavity length was close to the length of excited cone observed from the side images. The cone length was determined by the penetration depth L_p of pump light into the suspension. When the scattering mean free path l_s exceeded the absorption length at the pump wavelength, L_p was determined solely by absorption of pump light. This could explain the experimental observation that the wavelength spacing of lasing peaks barely changed when the scattering mean free path l_s was varied by more than one order of magnitude. The cavity length L_c (or the penetration depth L_p) did not depend on l_s as long as l_s exceeded the absorption length. This result was confirmed by the side images of excited cones.

In the case of linear absorption, L_p was on the order of the (linear) absorption length l_a . However, the pumping in the lasing experiment was so intense that it saturated the absorption of dye molecules. The saturation photon flux density $I_s = 1/\sigma_f\tau_f$, where σ_f is

the fluorescence cross section and τ_f is the lifetime of dye molecules in the excited state. For Rhodamine 640 molecules, σ_f is of the order 10^{-16} cm², and τ_f 10^{-9} s. Thus, $I_s \sim 10^{25}$ cm⁻²s⁻¹. The typical pump pulse energy at the lasing threshold was ~ 0.1 μ J. From the pump pulse duration and pump spot size, we estimated that the incident pump photon flux density $I_p \sim 10^{27}$ cm⁻²s⁻¹, which was two orders of magnitude higher than I_s . Hence, at the lasing threshold the absorption of dye molecules near the front window of the cuvette was strongly saturated, and the penetration depth L_p was much longer than l_a . Our pump pulse was so short that the probability of a dye molecule being excited then deexcited and excited again during one pump pulse was negligible. Assuming every dye molecule inside the excited cone absorbed one pump photon per pulse, we estimated the cone length $L_p = E_p / (h\nu_p) / (D\pi r_p^2 / 3)$, where E_p is the incident pump pulse energy, h is the Planck constant, ν_p is the pump frequency, D is the density of dye molecules. For $E_p = 0.1$ μ J, $\lambda_p = 532$ nm, $D = 3.1 \times 10^{24}$ m⁻³, $r_p = 20$ μ m, we got $L_p = 236$ μ m. This value was close to the laser cavity length estimated from the wavelength spacing of lasing peaks, $L_c = 265$ μ m.

To confirm $L_c \sim L_p$, we changed L_p by varying the dye concentration. The higher the dye concentration, the shorter the penetration depth. If $L_c \sim L_p$, the spacing of lasing peaks $\Delta\lambda$ should increase. Figure 8(a) shows the single shot lasing spectra from three solutions of $M = 3, 5, 10$ mM. The particle density ρ was fixed at 3×10^9 cm⁻³. It was evident that the spacing of lasing peaks increased at higher dye concentration. Images of the excited cones in the inset of Fig. 8(b) directly show that the excited cone was longer in the solution of lower dye concentration. Figure 8(b) plots the spectral correlation functions for the three spectra in 8(a). From them we extracted $\Delta\lambda = 0.34, 0.48, 0.96$ nm for $M = 3, 5, 10$ mM. This result confirmed that the laser cavity length was determined by the pump penetration depth. Hence, the laser cavity was located in the excited cone, and the cavity length was approximately equal to the cone length.

The experimental analysis suggested that the laser cavity in the weakly-scattering dye solution resembled a Fabry-Perot cavity with the “mirrors” at the tip and base of the excited cone. But what made of the mirrors in the dilute colloidal suspension? The experiments presented earlier in this section already ruled out the front and back windows of the cuvette as the mirrors. The mirrors could not be formed by the nonlinear change of refractive index (both its real and imaginary parts) of the dye solution under intense pumping, otherwise

lasing would have occurred also in the neat dye solution without particles. Another possibility is that the particles aggregated in the solution to form large clusters that served as mirrors. We monitored the solution during the experiment by imaging it onto a CCD camera through a side window of the cuvette. No clusters of size larger than $1\mu\text{m}$ were observed in the pumped solution. To remove the clusters smaller than $1\mu\text{m}$, we passed the solution through a $0.8\mu\text{m}$ pore-size filter paper. After the filtering, lasing phenomena remained the same. We also tried other particles such as ZnO and SiO₂ in different solvents like methanol and DEG. Our previous studies confirmed the particles did not aggregate in some of these solutions where we observed lasing. Therefore, the mirrors were not clusters of particles. Another candidate was bubbles or shock waves that were generated by the pump pulse^{17,18,19}. We indeed observed bubbles in the solution when the pump beam was strong enough and its focal spot was close to the front window of the cuvette. However, when the bubbles were big enough to be seen with our imaging apparatus, lasing peaks disappeared. Hence, big bubbles did not facilitate lasing. Small bubbles, which were invisible, might be generated when the pumping was not very high. Such bubbles were usually generated at the focal spot of the pump beam where the pump intensity was the highest. Thus the bubble formation should be sensitive to the distance between the focal spot and the front window, which affected the pump intensity at the focal spot due to absorption in the solution. However, the lasing behavior remained the same when we shifted the focal spot by moving the lens. This result eliminated the possibility of small bubbles contributing to lasing. All the experimental results led us to the speculation that the coherent feedback for lasing came from the particles in the solution. More specifically, the feedback could come mainly from the particles located near the tip and base of the excited cone.

In the dilute suspensions of particles in which lasing could be realized, the gain volume had a cone shape and the cone length was shorter than the scattering mean free path. If we considered only one photon, it most likely would not be scattered as it traveled from one end of the cone to the other. However, the intense pumping generated a huge number of emitted photons. Despite the low probability of *one* photon being scattered, a significant number of emitted photons were scattered by the particles inside the excited cone. Some of them were scattered backwards, providing feedback for lasing along the cone. Such weak feedback was strongly amplified due to high optical gain. The longer the path length, the stronger the amplification. Thus the light backscattered by the particles near one end of the cone

experienced the most amplification as it traveled to the other end of the cone. Therefore the feedback could be dominated by the particles located near the two ends of the excited cone. To support this conjecture, we performed numerical simulations which will be presented in the next section.

III. NUMERICAL SIMULATION

Several models were set up in the theoretical studies of stimulated emission in active random media, e.g. the diffusion equation with gain^{20,21}, the Monte Carlo simulation^{22,23}. These models calculated light intensity instead of electromagnetic field, thus they ignored the interference effect. Although it is usually weak in the diffusive regime, the interference effect is not always negligible. One example is the coherent backscattering. The interference between the counter-propagating light enhances the backscattered intensity by a factor of two. In the presence of optical gain, coherent amplification can strongly enhance the interference effect. Thus it may not be neglected even when light scattering is weak.

To include the interference effect, we directly calculated the electromagnetic field in a random medium by solving the Maxwell's equations using the finite-difference time-domain (FDTD) method²⁴. The optical gain was modeled as negative conductance

$$\sigma(\omega) = -\frac{\sigma_0/2}{1 + i(\omega - \omega_0)T_2} - \frac{\sigma_0/2}{1 + i(\omega + \omega_0)T_2}. \quad (1)$$

σ_0 determined the gain magnitude, ω_0 and $1/T_2$ represented the center frequency and width of the gain spectrum, respectively. The absence of gain saturation in Eq. 1 was not crucial as we intended to find the lasing modes just above the threshold. A seed pulse with broad spectrum was launched at $t = 0$ to initiate the amplification process. The lasing threshold was defined by the minimum gain coefficient (σ_0) at which the electromagnetic field oscillation built up in time. To shorten the computing time, we simulated lasing in two-dimensional systems. In order to model the elongated gain volume in the experiment, optical gain was introduced to a strip of length L_p and width W_p . The refractive index was set at 1.0 both inside and outside the strip. Dielectric cylinders of radius 100 nm and refractive index 2.0 was placed randomly in the strip as scattering centers. The strip dimension was much smaller than the experimental value due to the limited computing power. Consequently, the number of cylinders inside the strip was reduced to keep the system in

the weak scattering regime.

At the end of last section, we conjectured that the coherent feedback for lasing resulted mainly from the particles located near the tip and base of the excited cone. In the dilute suspension of particles, there was probably only one particle located at the tip of the cone. One question was whether the backscattering of a single particle could provide enough feedback for lasing. To answer this question, we considered there were only two particles in the gain strip, one on each end, in the numerical simulation. The total system size was $16 \mu\text{m} \times 8 \mu\text{m}$, and the gain strip $8 \mu\text{m} \times 4 \mu\text{m}$. At the system boundary, there was a perfectly matched absorbing layer. As shown in Fig. 9(a), two cylinders of radius 100 nm, placed at the two ends of the gain strip, had a separation of $8 \mu\text{m}$. When the gain coefficient σ_0 was above a threshold value, we observed lasing oscillation in the two-scatterer cavity. The spatial distribution of lasing intensity was plotted in Fig. 9(b). It revealed that lasing occurred along the strip with the feedback from the two particles. The spatial nonuniformity of laser intensity distribution was caused by beating of multiple lasing modes, which could be seen in the emission spectrum in Fig. 9(c). The spectrum was obtained by Fourier transform of the electric field, and the lasing modes were equally spaced in frequency. We varied the separation between the two scatterers, and the frequency spacing of lasing modes changed accordingly. The shorter the particle separation, the larger the mode spacing. These results illustrated lasing in the resonator composed of only two scatterers.

In 1998, Wilhelmi proposed a laser composed of two Rayleigh scatterers with gain medium in between²⁵. We generalized the Rayleigh scatterers to Mie scatterers and derived the lasing threshold condition for the two-particle cavity:

$$\frac{\sigma_b}{L_c^2} e^{g_e L_c} = 1. \quad (2)$$

σ_b was the backscattering cross section of one particle, which depended on the particle size, refractive index and incident light wavelength. L_c was the cavity length which was equal to the separation between the two scatterers. g_e was the threshold gain coefficient for lasing. Eq.(2) reveals two competing factors in determining the lasing threshold. On one hand, the optical feedback from one particle to the other is inversely proportional to L_c^2 . The farther apart the two particles, the higher the loss of the two-scatterer cavity. On the other hand, light amplification grows exponentially with L_c . When the optical gain is high, the exponential growth of amplification dominates over the quadratic increase of cavity loss. The

lasing threshold decreases with increasing L_c . Hence, the resonator with the lowest lasing threshold is composed of two particles with the largest separation inside the gain volume. In other words, the lasing cavity length is equal to the largest dimension of the gain volume. Experimentally, tight focusing of the pump beam created a cone-shaped gain volume in a dilute suspension of particles. The two particles furthest apart were located at the base and tip of the cone. The lasing cavity length was equal to the cone length. The lasing modes were longitudinal modes of the two-particle cavity. Hence they were equally spaced in frequency with the spacing $\Delta\nu = c/2n_eL_c$, where c was the speed of light and n_e was the effective refractive index of gain medium between the two particles. The regular mode spacing was consistent with our numerical simulation which confirmed Wilhelmi's theory of such a microscopic laser.

Although the equally spaced lasing modes were expected, the directional lasing output from a two-scatterer cavity was a surprise to us. In our numerical simulation, the near-field to far-field transformation of electric field gave the output laser intensity as a function of polar angle. Figure 9(d) shows the numerical data for three gain strips of length $L_p = 4, 8, 16 \mu\text{m}$. The strip width W_p was fixed at $4 \mu\text{m}$. The two scatterers were always placed at the ends of the strip. From the envelop of the far-field intensity distribution, we obtained the angular width of the output laser beam. It decreased as the aspect ratio of the gain strip L_p/W_p increased. Similar results were obtained when we varied W_p and kept L_p constant. These results indicated that the output from a two-particle cavity laser cannot be simply regarded as scattering of a plane wave by a single particle. The formation of coherent lasing modes relied not only on the geometry of the scatterers, but also on the shape of gain strip. Hence, the directionality of lasing output depended on the aspect ratio of the gain strip.

Experimentally there were particles not only at the ends of the excited cone, but also in the middle. To find out what happened when there were additional scatterers in between the two near the ends, in the numerical simulation we randomly placed a few cylinders inside the gain strip in addition to the two at the ends. Figure 10(a) shows the spatial distribution of laser intensity with four additional cylinders inside the gain strip of dimension $8 \times 4 \mu\text{m}$. Despite the presence of additional scatterers, lasing still occurred in the direction parallel to the strip. The lasing spectrum in Fig. 10(b) again exhibited almost equally spaced lasing peaks. The peak spacing was close to that with only two cylinders at the strip ends. This numerical result confirmed our speculation that the contributions to lasing for the

scatterers near the strip ends dominated over those from the scatterers in the middle. For a simple illustration, let us consider the photons emitted near one end of the gain strip, e.g., the left end, and propagating along the strip to the right. The stimulated emission led to an exponential growth of photon number with the path length. When they reached one scatterer inside the strip, a small percentage of the photons were scattered, while the majority continued propagating. The longer the propagation path, the larger the number of photons. As long as the strip length was less than the scattering mean free path, the number of photons reaching the right end of the strip was the largest, so was the number of photons scattered by the particle near this end. The backscattered photons were amplified as they propagated along the gain strip to the left end. Some of these photons were scattered into other directions by the particles on the way. This linear scattering loss was offset by the high optical gain which led to exponential increase of photon number. The light backscattered from the particle at the right end was amplified the most among all the backscattered waves reaching the left end, because of its longest path in the gain strip. Therefore, the feedbacks from the scatterers near the ends of gain strip were much stronger than those from the particles in the middle. As a result, the lasing frequencies were mainly determined by the distance between the scatterers nears the two ends of the gain strip, and the lasing modes were almost equally spaced in frequency. Experimentally, when the number of scatterers increased, the pump strip was shortened due to increased scattering of pump light. Thus the lasing threshold rose. A further increase of scatterer density destroyed the regular spacing of lasing modes as multiple scattering became dominant.

Although in the dilute suspension there was probably only one particle at the tip of the excited cone, there were more particles at the cone base whose dimension exceeded the average distance between the particles. For example, when the particle density $\rho = 5 \times 10^8 \text{ cm}^{-3}$ and pump spot diameter $\sim 40 \mu\text{m}$, there were at least ten particles near the base of the excited cone. To simulate this experimental situation, we placed ten scatterers randomly near one end of the gain strip and only one scatterer at the other end. Figure 10(c) shows the spatial distribution of laser intensity. The lasing peaks were almost equally spaced in frequency, as shown in Fig. 10(d). The peak spacing was close to that with only two scatterers in the strip, one on either end. It suggested that the feedback from the ten scatterers near one end of the gain strip was equivalent to that from one located somewhere close to this end, as far as the lasing frequencies were concerned. Hence, the frequency

spacing of lasing peaks scaled inversely with the length of gain strip.

IV. DISCUSSION AND CONCLUSION

Although our numerical simulations were performed on 2D systems with smaller dimensions, the conclusions obtained were in agreement with the 3D systems of larger dimensions in our experiment. They presented a qualitative explanation for the lasing behaviors in the weakly-scattering systems. When the scattering mean free path exceeded the size of gain volume, lasing oscillation built up in the direction of strongest amplification, i.e., the direction in which the gain volume was most extended. This behavior was similar to that of amplified spontaneous emission in the weak scattering regime²⁶. The fundamental difference from the ASE was the existence of feedback that originated from the backscattered light. The extreme weakness of feedback was compensated by high optical gain due to intense pumping. As pointed by Kumar and coworkers, the statistically rare sub-mean-free-path scattering could be made effective by strong amplification²⁷. They demonstrated lasing in active, sub-mean-free-path-sized systems with dense, random, weak scatterers. The feedback came from *all* the scatterers in the system. In our case the feedback came mainly from the scatterers near the ends of the gain strip, because it was selectively amplified due to the long propagation path in the gain volume. However, at very low particle density, the chance of having particles near the ends of a gain strip was reduced, thus the lasing threshold was increased. Moreover, when the particle density was high, the shape of gain volume was changed to a hemisphere. The reduction of path length in the gain volume led to an increase of lasing threshold.

A few years ago, Vardeny and coworkers observed lasing oscillation along a pump strip^{5,6}. They attributed the feedback to weak backscattering occurring repeatedly along the entire strip. In other words, the process of multiple scattering supplied the distributed feedback for lasing. In our case, the feedback was not distributed over the entire excited cone, but came mainly from the scatterers near the cone ends as a result of weak scattering and strong amplification. Thus the lasing modes had constant frequency spacing, which depended on the cone length. Our previous numerical study¹⁰ illustrated that the lasing modes can be completely different from the quasimodes of the passive systems in the case of local pumping. The absorption of emitted light outside the pumped region effectively reduces the system

size, and the lasing modes are confined in the pumped region. In this work, we suggested that the lasing modes may also differ from the quasimodes of the *reduced* system without gain or absorption. The former were formed mainly by scattering of particles near the boundary of the reduced system in the presence of high gain, while the latter were formed by scattering of all particles inside the reduced system in the absence of gain and absorption.

In summary, we observed lasing with coherent feedback in dye solutions containing a small amount of nanoparticles under confined intense optical pumping. The focused pump beam created a cone-shaped gain volume. The cone length was determined by the absorption of dye molecules since optical scattering was very weak. The laser output was in the direction parallel to the cone. The lasing modes were almost equally spaced in frequency, and their spacing was inversely proportional to the cone length. Despite the weak scattering, the laser cavity was confined to the excited volume of dimension less than the scattering length. It was a result of interplay between strong amplification of emission inside the excited volume and reabsorption of emitted light outside it. Hence, even in a weakly-scattering system, the lasing modes may be localized in a small region by local pumping. Moreover, the shape of gain volume determined the orientation of laser cavities. In the ballistic regime where the size of gain volume was less than the scattering mean free path, lasing occurred along the direction in which the gain volume was most stretched for maximum amplification. It led to directional laser output. The extreme weakness of feedback originating from the backscattering was offset by the strong amplification under intense pumping. The high optical gain selectively amplifies the feedback from the scatterers near the ends of the pump strip due to long propagation path inside the gain region. Thus the frequency spacing of lasing modes was determined by the maximum dimension of the gain volume. These results illustrated that it is possible to control the lasing frequencies and output directionality of random lasers by varying the pumping geometry, the scattering mean free path, the absorption length at excitation and emission wavelengths.

The authors acknowledge Dr. Christian Vanneste for stimulating discussion. This work was supported by the National Science Foundation under the grant no. ECS-0244457 and

-
- ¹ R. V. Ambartsumyan, N. G. Basov, P. G. Kryukov, and V. S. Letokhov, *IEEE J. Quant. Electron.* **QE-2** 442 (1966).
- ² H. Cao, *Waves in Random Media* **13**, R1 (2003).
- ³ H. Cao, *J. Phys. A: Math. Gen.* **38**, 10497 (2005), and reference therein.
- ⁴ H. Cao, J. Y. Xu, S.-H. Chang, S. T. Ho, E. W. Seelig, X. Liu, and R. P. H. Chang, *Phys. Rev. Lett.* **84**, 5584 (2000).
- ⁵ S. V. Frolov, Z. V. Vardeny, A. Z. Zakhidov, and R. H. Baughman, *Opt. Commun.* **162**, 241 (1999).
- ⁶ S. V. Frolov, M. Shkunov, A. Fujii, K. Yoshino, and Z. V. Vardeny, *IEEE J. Quantum Electron.* **36**, 2 (2000).
- ⁷ Y. Ling, H. Cao, A. L. Burin, M. A. Ratner, C. Liu, R. P. H. Chang, **64**, 063808 (2001).
- ⁸ R. C. Polson, M. E. Raikh, and Z. V. Vardeny, *C. R. Acad. Sci. Paris IV* **3**, 500 (2002).
- ⁹ R. C. Polson, and Z. V. Vardeny, *Phys. Rev. B* **71** 045205 (2005).
- ¹⁰ A. Yamilov, X. Wu, H. Cao, and A. Burin, *Opt. Lett.* **30**, 2430 (2005).
- ¹¹ F. A. Korolev, G. V. Abrosimov, A. I. Odintsov, and V. P. Yakunin, *Opt. Spectrosc.* **28**, 540 (1970); F. A. Korolev, V. I. Atroshchenko, S. A. Bakhramov, and V. I. Odintsov, *ibid* **34** 591 (1973).
- ¹² V. I. Ishchenko, V. N. Lisitsyn, A. M. Razhev, S. G. Rautian, and A. M. Shalagin, *JETP Lett.* **19** 346 (1974).
- ¹³ F. A. Korolev, A. I. Odintsov, N. G. Turkin, and V. P. Yakunin, *Sov. J. Quant. Electron.* **5** 237 (1975).
- ¹⁴ V. Ye. Brazovsky and V. N. Lisitsyn, *Appl. Phys.* **18** 421 (1979).
- ¹⁵ Z. Bor, S. Szatmari, and A. Muller, *Appl. Phys. B* **32**, 101 (1983).
- ¹⁶ P. Sperber, W. Spangler, B. Meier and A. Penzkofer, *Opt. Quantum Electron.* **20**, 395 (1988).
- ¹⁷ A. A. Chastov and O. L. Lebedev, *Sov. Phys. JETP* **31** 455 (1970).
- ¹⁸ V. I. Bezrodnyi, V. I. Vashchuk, and E. A. Tikhonov, *Sov. Phys. Tech. Phys.* **23** 89 (1978).
- ¹⁹ A. Vogel, K. Nahen, D. Theisen, and J. Noack, *IEEE J. Sel. Topic. Quant. Electron.* **2** 847 (1996).

- ²⁰ D. S. Wiersma and A. Lagendijk, *Phys. Rev. E* **54**, 4256 (1996).
- ²¹ S. John, and G. Pang, *Phys. Rev. A* **54**, 3642 (1996).
- ²² G. A. Berger, M. Kempe, and A. Z. Genack, *Phys. Rev. E* **56**, 6118 (1997).
- ²³ S. Mujumdar, M. Ricci, R. Torre, and D. W. Wiersma, *Phys. Rev. Lett.* **93**, 053903 (2004).
- ²⁴ A. Taflove and S. C. Hagness, *Computational Electrodynamics* (Artech, 2000).
- ²⁵ B. Wilhelmi, *Microwave and Optical Tech. Lett.* **17**, 111 (1998).
- ²⁶ D. S. Wiersma, M. P. van Albada, and A. Lagendijk, *Nature (London)* **373**, 203 (1995).
- ²⁷ B. R. Prasad, H. Ramachandran, A. K. Sood, C. K. Subramanian, and N. Kumar, *Appl. Opt.* **36**, 7718 (1997).

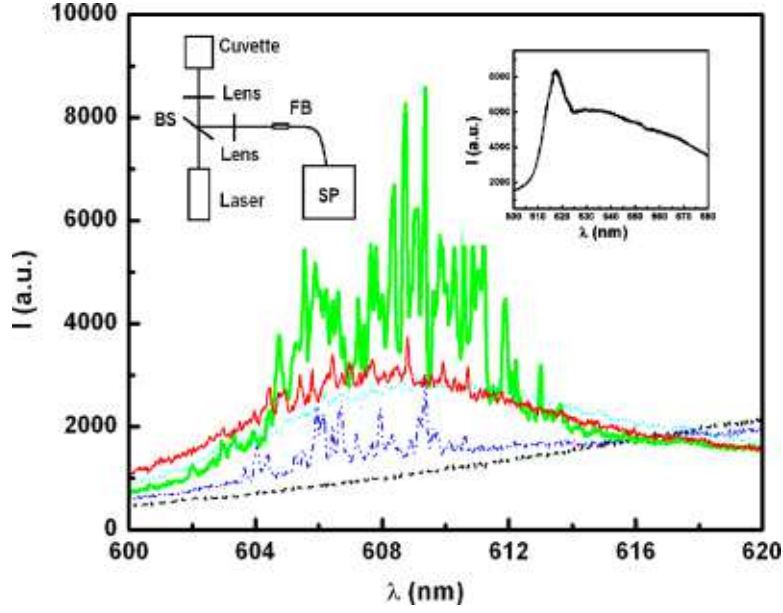


FIG. 1: Spectra of emission from DEG solutions of Rhodamine 640 (5 mM) and TiO_2 particles. The particle density $\rho = 0$ (dotted curve), $1.87 \times 10^8 \text{ cm}^{-3}$ (thin solid curve), $1.87 \times 10^9 \text{ cm}^{-3}$ (thick solid curve), 4: $1.3 \times 10^{10} \text{ cm}^{-3}$ (dot-dot-dashed curve), 5: $5.0 \times 10^{10} \text{ cm}^{-3}$ (dashed curve). All spectra were taken at the same pump pulse energy $0.4 \mu\text{J}$. Each spectrum was integrated over 25 shots. Left inset is the skemetic of our experimental setup, BS: beam splitter, SP: spectrometer, FB: fiber bundle. Right inset is the emission spectrum shows the ASE peak. $\rho = 5.0 \times 10^{10} \text{ cm}^{-3}$. The pump pulse energy is $1.2 \mu\text{J}$.

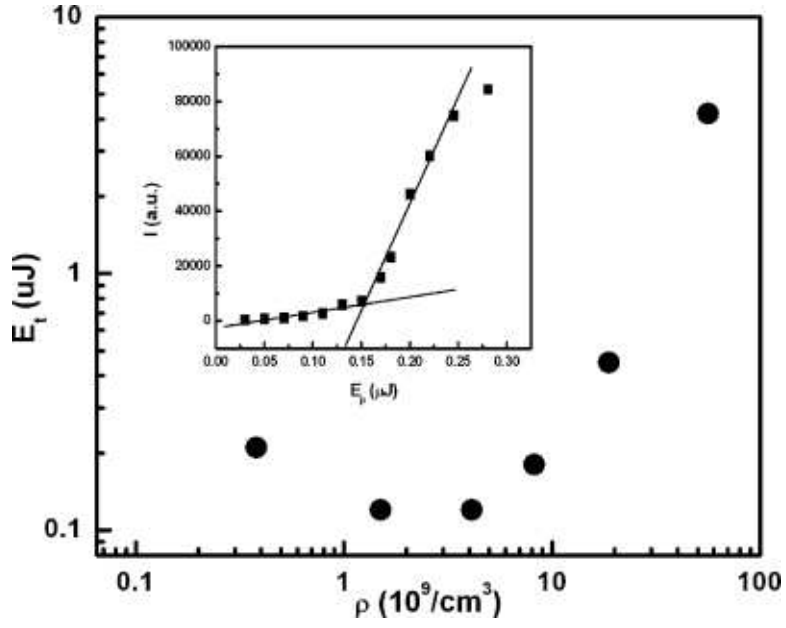


FIG. 2: The threshold pump pulse energy E_t as a function of the TiO_2 particle density ρ . The concentration of Rhodamine 640 in DEG is 5 mM. The inset is a plot of the emission intensity I versus the pump pulse energy E_p for the suspension with $\rho = 3.0 \times 10^9 \text{ cm}^{-3}$.

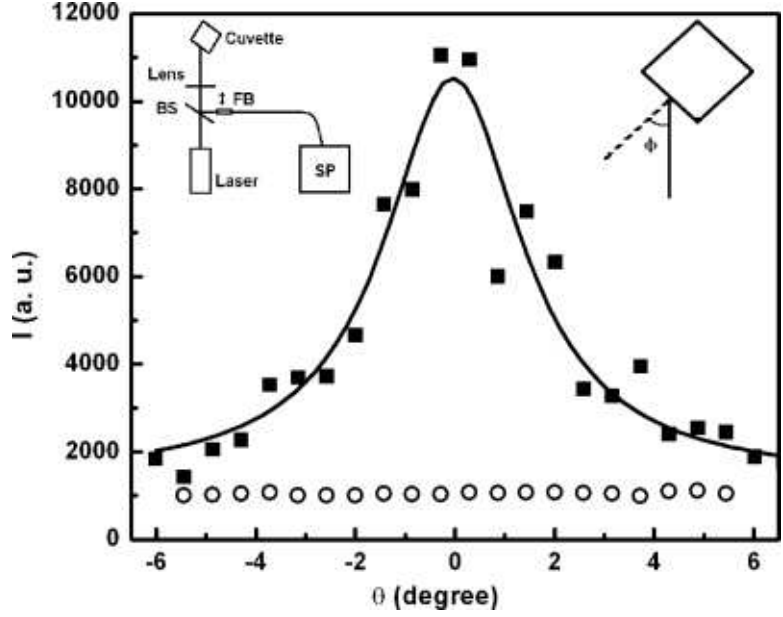


FIG. 3: The angular distribution of output emission intensity from DEG solutions of 5 mM Rhodamine 640 and $3.0 \times 10^9 \text{ cm}^{-3}$ (solid square) and $5.0 \times 10^{10} \text{ cm}^{-3}$ (open circle) TiO_2 particles. The solid line is a Gaussian fit of output laser beam. $\theta = 0$ corresponds to the backward direction of pump beam. Left inset is a sketch of experimental setup, BS: beam splitter, SP: spectrometer, FB: fiber bundle. Right inset shows the angle ϕ between the pump beam and the normal to the front window of the cuvette.

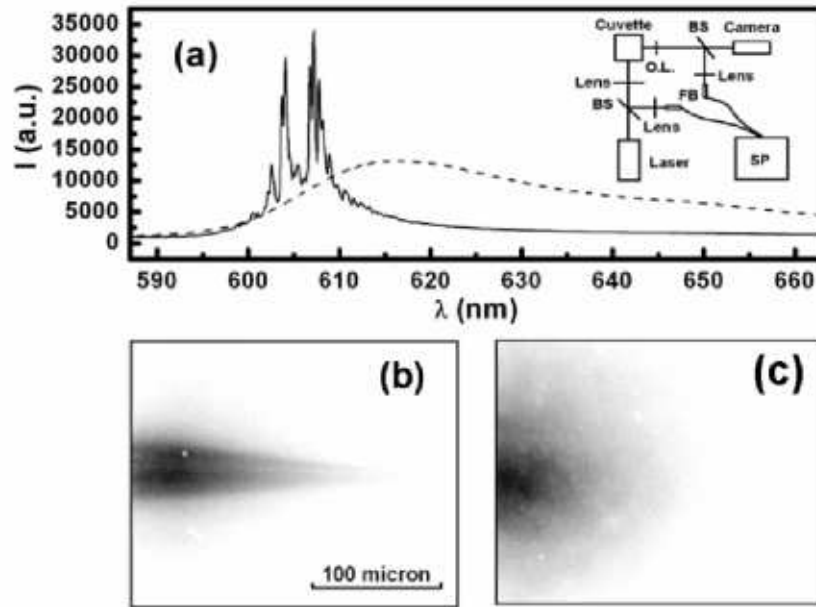


FIG. 4: (a): Spectra of emission through the side window (dashed curve) and front window (solid curve) of the cuvette. The inset is a sketch of the experimental setup, BS: beam splitter, SP: spectrometer, FB: fiber bundle. (b): Side image of excited region in DEG solution of 5 mM Rhodamine 640 and $3.0 \times 10^9 \text{ cm}^{-3}$ TiO_2 particles. The pump pulse energy is $0.2 \mu\text{J}$. (c): Side image of excited region in DEG solution of 5 mM Rhodamine 640 and $5.0 \times 10^{10} \text{ cm}^{-3}$ TiO_2 particles. The pump pulse energy is $1.2 \mu\text{J}$.

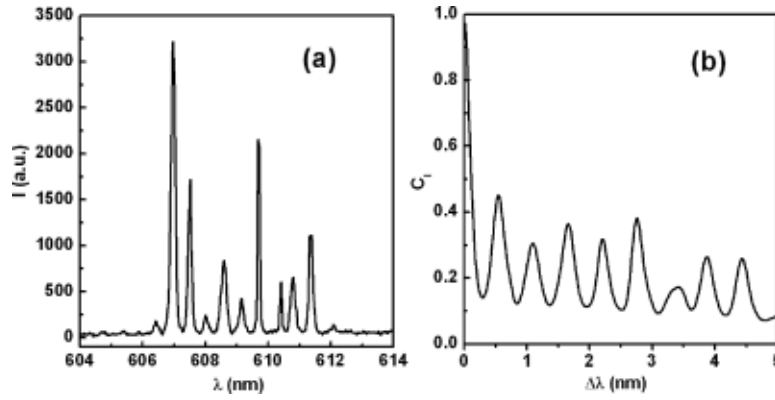


FIG. 5: (a): A single shot emission spectrum from DEG solution of 5 mM Rhodamine 640 and $1.87 \times 10^9 \text{ cm}^{-3}$ TiO_2 particles. The pump pulse energy is $0.2 \mu\text{J}$ pumping. (b): Spectral correlation function computed for the spectrum in (a).

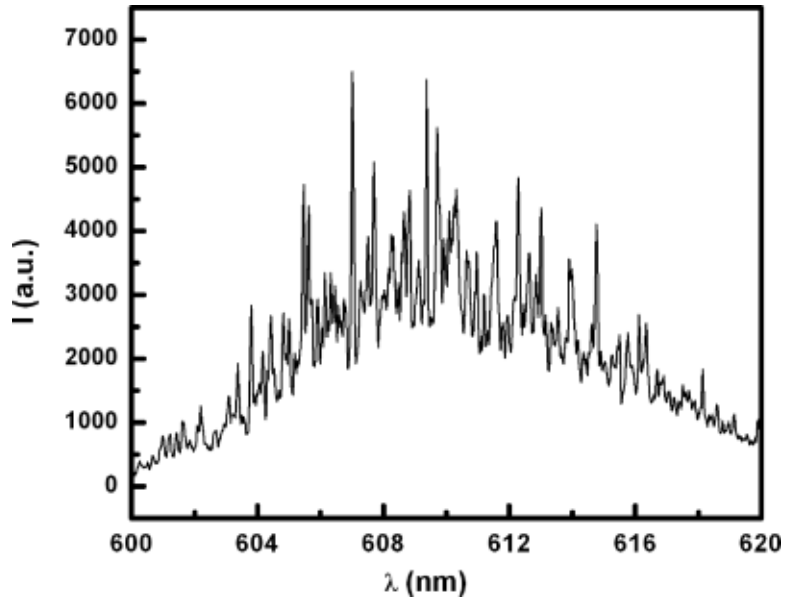


FIG. 6: A single shot emission spectrum from the DEG solution of 5 mM Rhodamine 640 without any particles. The pump pulse energy is $0.3 \mu\text{J}$ pumping.

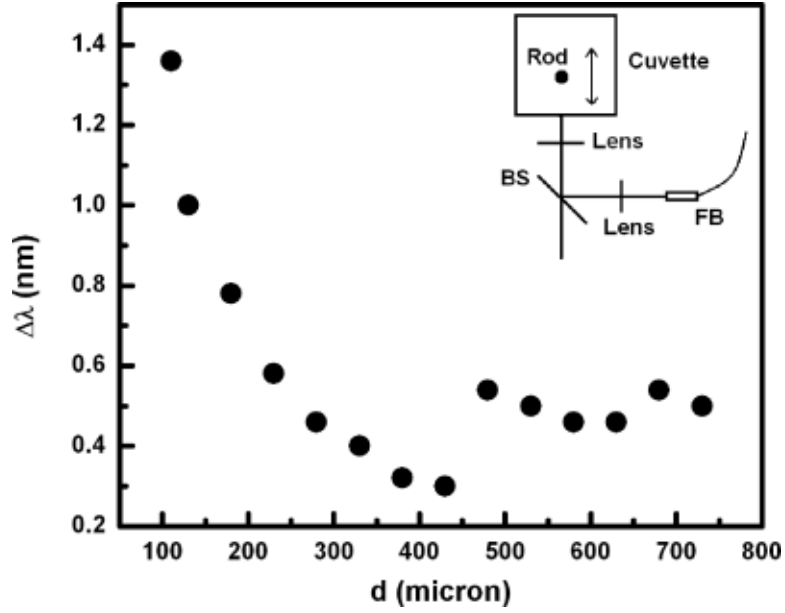


FIG. 7: The wavelength spacing $\Delta\lambda$ of lasing modes as a function of the distance d between the metallic rod and the cuvette front window. The concentration of Rhodamine 640 in DEG is 5 mM, and the TiO_2 particle density is $3.0 \times 10^9 \text{ cm}^{-3}$. The pump pulse energy is $0.2 \mu\text{J}$. The inset is a sketch of experimental setup. BS: beam splitter, FB: fiber bundle.

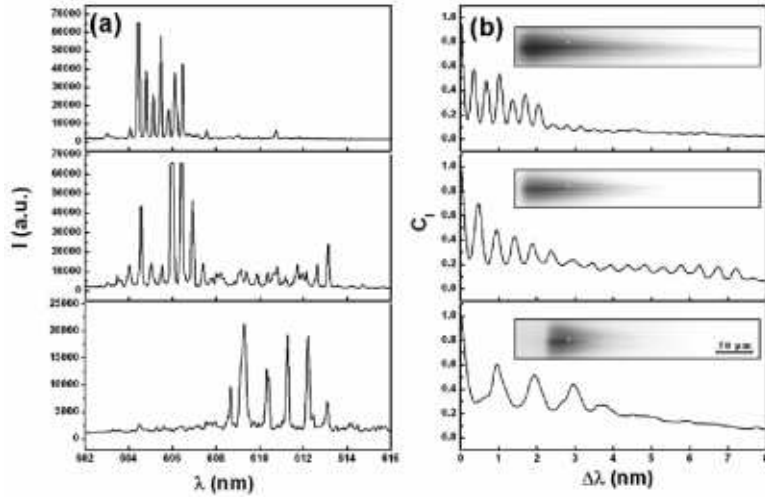


FIG. 8: (a): Single shot emission spectra from colloidal solution of $3.0 \times 10^9 \text{ cm}^{-3}$ TiO_2 particles. The molarity of Rhodamine 640 in DEG is (from top to bottom) 3 mM, 5 mM, and 10 mM. (b) Spectral correlation functions of the single shot emission spectra in (a). Insets are side images of pumped region for in each solution.

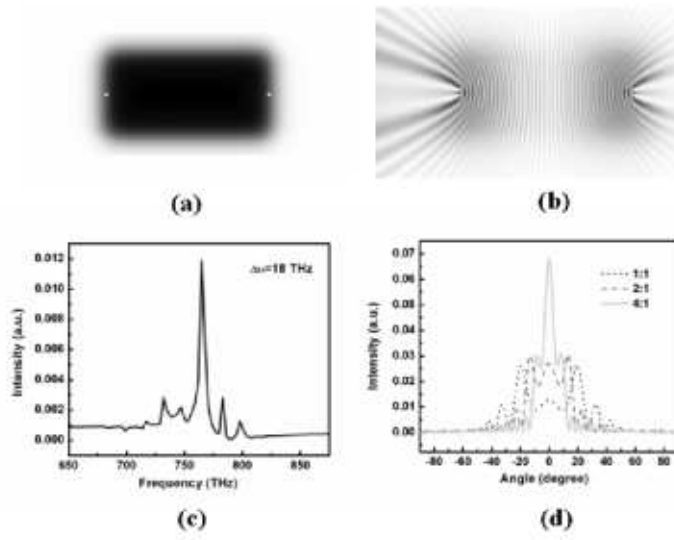


FIG. 9: (a) Geometry of a 2D system in our numerical simulation. The system size is $16 \mu\text{m} \times 8 \mu\text{m}$. The gain strip in the center has a dimension of $8 \mu\text{m} \times 4 \mu\text{m}$. Two cylinders of radius 100 nm are located on both ends of the gain strip. (b) Spatial distribution of laser intensity. (c) Emission spectrum features multiple lasing modes that are almost equally spaced in frequency. (d) Far-field intensity of laser emission as a function of polar angle. The zero degree corresponds to the direction parallel to the gain strip. The dimensions of the gain strip are $4 \mu\text{m} \times 4 \mu\text{m}$ (dotted curve), $8 \mu\text{m} \times 4 \mu\text{m}$ (dashed curve), $16 \mu\text{m} \times 4 \mu\text{m}$ (solid curve).

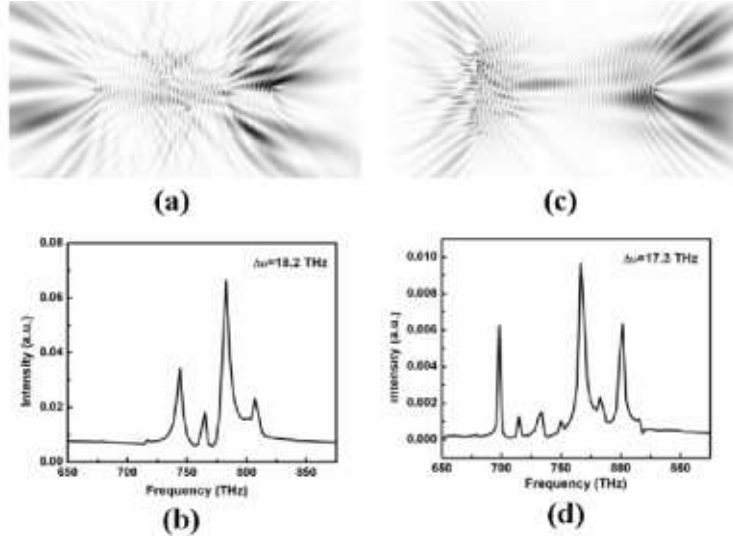


FIG. 10: (a) Spatial distribution of laser intensity with four scatterers randomly placed in between the two scatterers near the ends of gain strip. (b) Lasing spectrum corresponding to (a). (c) Spatial distribution of laser intensity with one scatterer on one end of the gain strip, and ten randomly placed scatterers near the other end. (d): Lasing spectrum corresponding to (c).